Available online at www.sciencedirect.com
ScienceDirect
Journal of Geodynamics 43 (2007) 200–213
JOURNAL OF GEODYNAMICS
http://www.elsevier.com/locate/jog

UNB application of Stokes–Helmert's approach to geoid computation

A. Ellmann *, P. Vaníček

Department of Geodesy and Geomatics Engineering, University of New Brunswick (UNB), P.O. Box 4400, E3B 5A3 Fredericton, New Brunswick, Canada

Received 4 November 2005; received in revised form 4 July 2006; accepted 18 September 2006

Abstract

Over the past two decades the so-called Stokes–Helmert method has been used for regional geoid determination at the University of New Brunswick (UNB). The present contribution summarizes the main principles of the UNB approach and successive theoretical developments. A two-space set-up is used for formulating the boundary value problem and defining gravity quantities, which would be appropriate for downward continuation from the Earth's surface to the geoid level. Focus of this paper is given on the topographical effects, which are formulated in their spherical form. UNB's solution of the Stokes boundary value problem employs a modified Stokes's formula in conjunction of the low-degree contribution of a global geopotential model (GGM). Various aspects at the regional geoid computations in the context of UNB's principles are illustrated by employing a new GRACE satellite mission based geopotential model for the numerical study. The new gravimetric geoid model is compared with local GPS-levelling data. Possible reasons of the detected discrepancies between the gravimetric geoid model and the control points are discussed.

Keywords: Gravimetric geoid; Boundary value problem; Topographic effects; Modified Stokes's formula

1. Introduction

The geoid as an equipotential surface of the Earth's gravity field plays an essential role in geosciencies and in many practical applications. In geodesy, it serves as the reference surface for topographic height and depth measurements.

The solution of the boundary value problem by Stokes's (1849) method requires gravity observations referred to the geoid as a boundary surface while in reality gravity measurements are taken at the topographic surface. Thus, to satisfy the boundary condition the gravity anomalies need to be downward continued to the geoid level. Downward continuation requires harmonicity of the quantities to be downward continued; thus a number of different corrections related to the existence of topography and atmosphere need to be accounted for very carefully. It is well known that the evaluation of topographical effects is one of the most serious limitations in precise geoid modeling nowadays. Therefore, the topographical effects need be rigorously formulated and evaluated using the spherical model of topography.

* Corresponding author. Present address: Department of Civil Engineering, Tallinn University of Technology, Ehitajate tee 5, 19086 Tallinn, Estonia. Tel.: +372 620 2603; fax: +372 620 2601.
E-mail addresses: artu.ellmann@ttu.ee (A. Ellmann), Vanicek@unb.ca (P. Vaníček).

0264-3707/$ – see front matter © 2006 Elsevier Ltd. All rights reserved.
doi:10.1016/j.jog.2006.09.019

One way of estimating the effect of topographical masses is to use Helmert's (1884) second condensation model. According to this model the Earth's topographical masses are replaced by an infinitesimal condensation layer on the geoid. To use this model, the real field quantities are first transformed into corresponding quantities in this model space which we call the Helmert space. So "Helmertised" a gravity field can be then decomposed into low- and high-frequency parts. Global geopotential models (GGM) are the most accurate source for the low-frequency information, whereas the short-wavelength information is obtained from the Stokesian integration. For practical considerations, the integration is limited to a circular cap around the computation points. Importantly, the Stokes kernel modification scheme is employed. This scheme mitigates the error in the contribution from the field in the remote zone which exists even though the contribution is rigorously evaluated from global geopotential model.

The theoretical principles of the UNB approach, successive theoretical and practical developments have been reported in dozens of scientific and professional papers by different authors. The authors of this paper were invited to summarize the main principles of the UNB geoid determination methods by the organizers of the geodesy and geodynamics sessions at the General Assembly of the European Geosciences Union, held in Vienna, in April 2005. Accordingly, the present contribution could be considered as an extended complement to the oral presentation. As such, it does not intend to compare the method in question with other contemporary (and to certain extent competitive) geoid determination methods. This task would require a throughout review of alternative methods. At the same time, due to limited space we could include to the present paper only the most important features of the UNB approach. Therefore, for more details of the UNB geoid determination approach the interested reader will be referred to relevant sources when appropriate. It should be noted that some underlying principles of the UNB approach and that of some other methods are already compared and discussed in the geodetic literature, see, e.g. Jekeli and Serpas (2003), Featherstone et al. (2004) and Sjöberg (2005).

The UNB approach is used not only in Canada but also by other institutions worldwide, often with some modifications. The theory behind the UNB approach has been empirically validated by a number of practical geoid computations. Recently launched dedicated gravimetric satellite missions (CHAMP and GRACE) have improved significantly the quality of the "satellite-only" component of global geopotential models. This fact allows us revisiting the selection of certain "practical" parameters in geoid determination as well. Therefore, among other relevant aspects in regional geoid modeling, the section of numerical investigations of this paper describes briefly a typical computational set-up for employing a recent GRACE-based geopotential model.

2. Boundary value problem and boundary values in the Stokes–Helmert scheme

2.1. Real space

Generally, the disturbing gravity potential $T(r, \Omega)$ is defined as a difference of the Earth's gravity potential $W(r, \Omega)$ and the normal gravity potential $U(r, \Omega)$ generated by a geocentric reference ellipsoid (e.g. GRS-80, see Moritz, 1992), i.e.

$$T(r, \Omega) = W(r, \Omega) - U(r, \Omega). \tag{1}$$

The geocentric position (r, Ω) of any point can be represented by the geocentric radius (r, Ω) and a pair of geocentric coordinates $\Omega = (\phi, \lambda)$, where ϕ and λ are the geocentric spherical coordinates. A note about the quantification to be used throughout this paper should be made. The region of interest of this study is the outer space of the geoid and the geoid itself. Thus, Eq. (1) and all subsequent expressions are valid for $r(\Omega) \geq r_g(\Omega)$, where $r_g(\Omega)$ is the geocentric radius of the geoid surface. For solving the geoid and related corrections the mathematical operations need often to be taken over the total solid angle $\Omega_0 = [\phi \in \langle -\pi/2, -\pi/2\rangle, \lambda \in \langle 0, 2\pi\rangle]$. The cases employing a different spatial domain will be outlined.

It is well known that the disturbing potential is harmonic in regions of zero density. If the topographic and atmospheric masses were completely absent, then T would be harmonic above the geoid surface, so that Laplace's equation is satisfied, i.e.

$$\nabla^2 T(r, \Omega) = 0. \tag{2}$$

where ∇^2 denotes the Laplace operator (Heiskanen and Moritz, 1967, p. 5).

If the values of the disturbing potential were known on the geoid, $T(r_g, \Omega)$, then the separation between the reference ellipsoid and the geoid could be obtained by the Bruns's formula (Bruns, 1878)

$$N(\Omega) = \frac{T(r_g, \Omega)}{\gamma_0(\phi)}, \tag{3}$$

where $\gamma_0(\phi)$ is the normal gravity (a function of latitude) on the reference ellipsoid. Since the disturbing potential cannot be measured directly then the boundary value problem of the third kind (Heiskanen and Moritz, 1967, p. 11) has to be formulated and solved. In geoid determination some type of gravity anomalies, referred to the geoid level, are serving as the boundary values of this problem. To find a relation between the disturbing potential and the gravity anomalies the radial derivative of the disturbing potential is introduced (cf. Eq. (1)):

$$\frac{\partial T(r, \Omega)}{\partial r} = \frac{\partial W(r, \Omega)}{\partial r} - \frac{\partial U(r, \Omega)}{\partial r}. \tag{4}$$

The above expression, evaluated at the Earth's surface, can be approximated by (Vaníček et al., 1999)

$$\left.\frac{\partial T(r, \Omega)}{\partial r}\right|_{r=r_t} \cong -g(r_t, \Omega) + \gamma(r_t, \Omega) + \varepsilon_{\delta g}(r_t, \Omega) = -\delta g(r_t, \Omega) + \varepsilon_{\delta g}(r_t, \Omega), \tag{5}$$

where the difference between the actual gravity $g(r_t, \Omega)$ and the normal gravity $\gamma(r_t, \Omega)$ is the gravity disturbance, $\delta g(r_t, \Omega)$, and $\varepsilon_{\delta g}(r_t, \Omega)$ is the ellipsoidal correction (due to replacing of the derivative with respect to ellipsoidal normal n by a more convenient radial derivative) to the gravity disturbance. The geocentric radius of the Earth's surface $r_t(\Omega)$ is obtained by adding the orthometric height $H^O(\Omega)$ to the $r_g(\Omega)$, i.e. $r_t(\Omega) \cong r_g(\Omega) + H^O(\Omega)$. This is an approximation, of course, since $H^O(\Omega)$ denotes the actual length of (somewhat curved) plumb-line between the geoid and the Earth surface. Considering the presently achievable geoid determination accuracy then its deviation from the geospherical radius can be safely neglected (but it can be accounted for in the most accurate computations). The used quantities are shown in Fig. 1.

Until the recent past (i.e. in the pre-GPS era) the gravity disturbance was not a measurable quantity. Therefore, the gravity disturbance has to be transformed into gravity anomaly, which is still the most widely available data type. In the modern context (Molodensky, 1945) the gravity anomaly $\Delta g(r_t, \Omega)$ is referred to the ground level and is related to $\Delta g(r_t, \Omega)$ by the following formula

$$\Delta g(r_t, \Omega) = \delta g(r_t, \Omega) + \gamma(r_t, \Omega) - \gamma[r_0(\phi) + H^N(\Omega)], \tag{6}$$

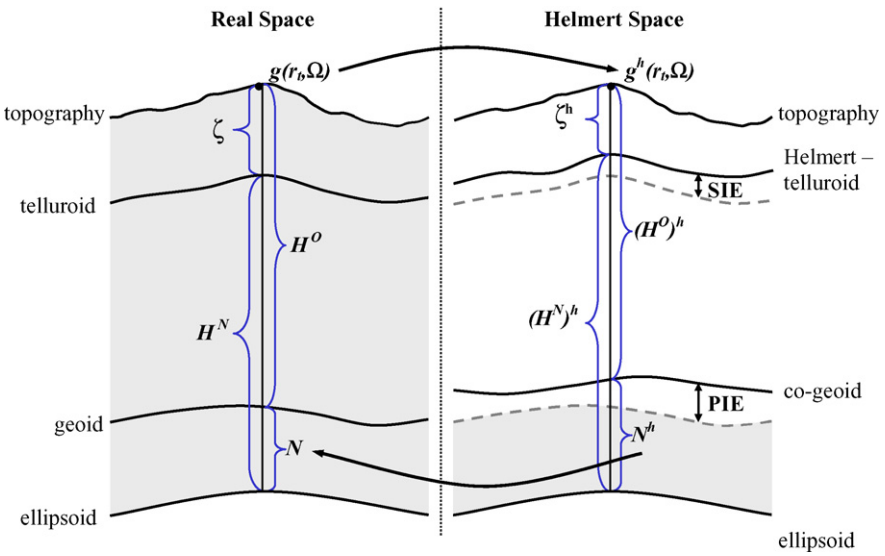

Fig. 1. The quantities involved in real and Helmert's spaces. See the text for more details.

where $H^{\mathrm{N}}(\Omega)$ is the normal height (Molodensky, 1945) and $r_0(\phi)$ is the geocentric radius (a function of latitude) of the surface of the reference ellipsoid.

Note that in Eq. (6) the normal gravity is referred to two different points in the space: $\gamma(r_{\mathrm{t}}, \Omega)$ to the surface and $\gamma[r_0(\phi)+H^{\mathrm{N}}(\Omega)]$ to the telluroid. This difference, after applying the Bruns's formula and spherical approximation, becomes (Vaníček and Martinec, 1994)

$$\gamma(r_{\mathrm{t}}\Omega) - \gamma[r_0(\phi) + H^{\mathrm{N}}(\Omega)] = \left.\frac{\partial\gamma(r,\phi)}{\partial n}\right|_{r=r_{\mathrm{t}}(\Omega)} \frac{T(r_{\mathrm{t}}, \Omega)}{\gamma[r_0(\phi) + H^{\mathrm{N}}(\Omega)]} = -\frac{2}{r_{\mathrm{t}}(\Omega)} T(r_{\mathrm{t}}, \Omega) - \varepsilon_n(r_{\mathrm{t}}, \Omega), \tag{7}$$

where $\partial\gamma/\partial n$ is the linear approximation of normal gravity gradient with respect to the normal n of the reference ellipsoid, and the ellipsoidal correction $\varepsilon_n(r_{\mathrm{t}}, \Omega)$ for the spherical approximation allows to replace "ellipsoidal" term by a more simple term $-(2/r(\Omega))T(r, \Omega)$. A detail derivation of the two ellipsoidal corrections (and their exact physical meaning along with numerical examples) is spelled out in Vaníček et al. (1999). Substituting Eqs. (5) and (7) into Eq. (6) the fundamental formula of physical geodesy takes the following form (Vaníček et al., 1999)

$$\Delta g(r_{\mathrm{t}}, \Omega) = -\left.\frac{\partial T(r, \Omega)}{\partial r}\right|_{r=r_{\mathrm{t}}(\Omega)} + \varepsilon_{\delta g}(r_{\mathrm{t}}, \Omega) - \frac{2}{r_{\mathrm{t}}(\Omega)} T(r_{\mathrm{t}}, \Omega) - \varepsilon_n(r_{\mathrm{t}}, \Omega). \tag{8}$$

This equation, formulated for the real space, can be applied in Helmert's space for the purpose of the computation of Helmert's gravity anomaly $\Delta g^{\mathrm{h}}(r_{\mathrm{t}}, \Omega)$.

2.2. Helmert space

Over the continental regions the geoid is mostly located inside the topographical masses. The gravity measurements are taken on the topographic surface. To satisfy the boundary condition the surface anomalies need to be continued downward to the geoid level. Downward continuation requires the function to be harmonic. Evidently, the presence of the topography violates the harmonicity condition. Therefore, in order to establish a harmonicity of the disturbing potential, the atmospheric and topographical masses have to be somehow accounted for.

This can be done by using Helmert's second condensation method, where the masses located above the geoid are condensed to a layer on the geoid—to define a new distribution of masses, which we think of as populating the above introduced Helmert space.

Principally, other topographic compensation models (e.g. as listed in Heiskanen and Moritz, 1967, Chapter 3) can also be considered at the geoid computations. For instance, in the Pratt-Hayford isostatic model the anomalies of density distribution are placed between some compensation level and the geoid. As a matter of fact, the Helmert second condensation model appears to be a limiting case of this isostatic reduction. A generalized Helmert condensation model is discussed in Heck (2003). However, due to relatively small indirect topographic effects the Helmert second condensation model is favoured for the UNB geoid determination approach.

The gravity field in Helmert's space is slightly different from the field in the real space. Helmert's gravity potential is defined as follows

$$W^{\mathrm{h}}(r, \Omega) = W(r, \Omega) - \delta V^{\mathrm{t}}(r, \Omega) - \delta V^{\mathrm{a}}(r, \Omega), \tag{9}$$

where the superscript h denotes the quantities given in the Helmert space, $\delta V^{\mathrm{t}}(r, \Omega)$ is the residual topographical potential, i.e. the difference between the potential of the topographical masses and the potential of the condensation layer

$$\delta V^{\mathrm{t}}(r, \Omega) = V^{\mathrm{t}}(r, \Omega) - V^{\mathrm{c}}(r, \Omega) \tag{10}$$

Similarly, the residual atmospheric potential $\delta V^{\mathrm{a}}(r, \Omega)$ is the difference between the potential of the atmospheric masses and the potential of the atmospheric condensation layer

$$\delta V^{\mathrm{a}}(r, \Omega) = V^{\mathrm{a}}(r, \Omega) - V^{\mathrm{ca}}(r, \Omega). \tag{11}$$

The Helmert disturbing potential can be then written as

$$T^{\mathrm{h}}(r, \Omega) = W^{\mathrm{h}}(r, \Omega) - U(r, \Omega) = T(r, \Omega) - \delta V^{\mathrm{t}}(r, \Omega) - \delta V^{\mathrm{a}}(r, \Omega). \tag{12}$$

It has been shown (Vaníček and Martinec, 1994) that the Helmert's disturbing potential is harmonic in every point outside the geoid—this is rather obvious from the fact that mass density above the geoid is equal to zero everywhere so that the Laplace equation

$$\nabla^2 T^{\mathrm{h}}(r, \Omega) = 0, \tag{13}$$

holds everywhere above the geoid ($r(\Omega) \geq r_{\mathrm{g}}(\Omega)$).

The question here is what are the appropriate gravity anomalies required for solving the geodetic boundary value problem in Helmert's space. The Helmert gravity $g^{\mathrm{h}}(r_{\mathrm{t}}, \Omega)$ is the negative radial derivative of the Helmert gravity potential, satisfying thus the usual definition of gravity. Considering also Eqs. (9)–(11) the Helmert gravity on the Earth's surface can be expressed via the actual gravity $g(r_{\mathrm{t}}, \Omega)$, by adding the direct topographical and atmospheric effects (both referred to the Earth's surface), $\delta A^{\mathrm{t}}(r_{\mathrm{t}}, \Omega)$ and $\delta A^{\mathrm{a}}(r_{\mathrm{t}}, \Omega)$, respectively (cf. Vaníček and Martinec, 1994):

$$g^{\mathrm{h}}(r_{\mathrm{t}}, \Omega) \approx -\frac{\partial W^{\mathrm{h}}(r_{\mathrm{t}}, \Omega)}{\partial r} \approx g(r_{\mathrm{t}}, \Omega) + \delta A^{\mathrm{t}}(r_{\mathrm{t}}, \Omega) + \delta A^{\mathrm{a}}(r_{\mathrm{t}}, \Omega), \tag{14}$$

Strictly speaking, the well-known relation $g = -\partial W/\partial r$ (see, e.g. Heiskanen and Moritz, 1967, Eq. 2-145), utilized in Eq. (14), is only an approximation, since the radial derivative is taken over the complete potential, rather than over a disturbing quantity (e.g. $\delta g = -\partial T/\partial r$). This is the main reason using the $\approx$ symbol in Eq. (14). However, this relation makes the link between the actual gravity (and corresponding gravity anomaly) to the Helmert gravity anomaly (see Eq. (17)) more transparent. Note also that this approximation affects similarly g and g^{h} and in the subsequent expressions we operate with disturbing quantities. Second, the derivative should be taken along the plumb-line (instead of r!), an ellipsoidal correction due this approximation will be introduced in Eq. (15)).

The direct effects are obtained by taking the radial derivative of the residual topographical and atmospheric potentials. Note also that the following sign conventions: $\delta A^{\mathrm{t}}(r_{\mathrm{t}}, \Omega) = (\partial \delta \mathrm{V}^{\mathrm{t}}(r_{\mathrm{t}}, \Omega))/\partial r$ and $\delta A^{\mathrm{a}}(r_{\mathrm{t}}, \Omega) = (\partial \delta \mathrm{V}^{\mathrm{a}}(r_{\mathrm{t}}, \Omega))/\partial r$ are adopted here. This is in accordance with the denotations in our earlier publications. More details on the estimation of $\delta A^{\mathrm{t}}(r_{\mathrm{t}}, \Omega)$ will be given in Section 3.

The Helmert gravity disturbance is defined as a sum of the negative radial gradient of the Helmert disturbing gravity potential and the ellipsoidal correction to the gravity disturbance (cf. Eq. (5)), i.e.

$$\delta g^{\mathrm{h}}(r_{\mathrm{t}}, \Omega) = -\frac{\partial T^{\mathrm{h}}(r_{\mathrm{t}}, \Omega)}{\partial r} + \varepsilon_{\delta g}(r_{\mathrm{t}}, \Omega) = g(r_{\mathrm{t}}, \Omega) - \gamma(r_{\mathrm{t}}, \Omega) + \varepsilon_{\delta g}(r_{\mathrm{t}}, \Omega) + \delta A^{\mathrm{t}}(r_{\mathrm{t}}, \Omega) + \delta A^{\mathrm{a}}(r_{\mathrm{t}}, \Omega), \tag{15}$$

By analogy with Eq. (8) the relationship between the boundary condition and the Helmert anomaly, $\Delta g^{\mathrm{h}}(r, \Omega)$, is given by

$$\begin{aligned}\Delta g^{\mathrm{h}}(r_{\mathrm{t}}, \Omega) &= -\left.\frac{\partial T^{\mathrm{h}}(r, \Omega)}{\partial r}\right|_{r=r_{\mathrm{t}}(\Omega)} + \varepsilon_{\delta g}(r_{\mathrm{t}}, \Omega) + \left.\frac{\partial \gamma(r, \Omega)}{\partial r}\right|_{r=r_{\mathrm{t}}(\Omega)} \frac{T^{\mathrm{h}}(r_{\mathrm{t}}, \Omega)}{\gamma[r_{\mathrm{o}}(\phi) + (H^{\mathrm{N}}(\Omega))^{\mathrm{h}}]} \\ &= -\left.\frac{\partial T^{\mathrm{h}}(r, \Omega)}{\partial r}\right|_{r=r_{\mathrm{t}}(\Omega)} + \varepsilon_{\delta g}(r_{\mathrm{t}}, \Omega) - \frac{2}{r_{\mathrm{t}}(\Omega)} T^{\mathrm{h}}(r_{\mathrm{t}}, \Omega) - \varepsilon_n(r_{\mathrm{t}}, \Omega).\end{aligned} \tag{16}$$

Importantly, the Helmert gravity anomaly can also be expressed via commonly used free-air anomalies $\Delta g(r, \Omega)$, see Eq. (6). Finally, one arrives at (Vaníček et al., 1999)

$$\begin{aligned}\Delta g^{\mathrm{h}}(r_{\mathrm{t}}, \Omega) = \Delta g(r_{\mathrm{t}}, \Omega) + \delta A^{\mathrm{t}}(r_{\mathrm{t}}, \Omega) + \frac{2}{r_{\mathrm{t}}(\Omega)} \delta V^{\mathrm{t}}(r_{\mathrm{t}}, \Omega) + \delta A^{\mathrm{a}}(r_{\mathrm{t}}, \Omega) \\ + \frac{2}{r_{\mathrm{t}}(\Omega)} \delta V^{\mathrm{a}}(r_{\mathrm{t}}, \Omega) + \varepsilon_{\delta g}(r_{\mathrm{t}}, \Omega) - \varepsilon_n(r_{\mathrm{t}}, \Omega).\end{aligned} \tag{17}$$

In the Helmert space the product of Helmert anomaly and geocentric radius, $\Delta g^{\mathrm{h}} \cdot r$, is harmonic (Vaníček et al., 1996a). Such field (gravity anomaly multiplied by r) can be continued downward to the geoid level.

In Eq. (17) the second and third terms on the right-hand side are the direct and secondary indirect topographic effects on the gravitational attraction. The non-topographical corrections to the Helmert gravity anomaly are as follows: direct atmospheric effect, secondary indirect atmospheric effect, ellipsoidal correction for the gravity disturbance and

ellipsoidal correction for the spherical approximation. The effect of the two ellipsoidal corrections on the geoidal heights may approach in some regions a dm-level (Vaníček et al., 1999). This in good agreement with a study of Ardalan and Grafarend (2001), who detected the discrepancies between the spherical approximation (i.e. without the ellipsoidal corrections) and the ellipsoidal Bruns's formula reaching up to 6.4 cm within a test area in Germany.

Principally, the ellipsoidal corrections can also be considered at the computation of the topography-related effects. As is advocated by Novák and Grafarend (2005) it could be appealing to express also the topographic/condensation potentials and their derivatives in a more complex way, namely in the form of ellipsoidal approximations. They propose decomposing the evaluation of each topographical effect into two parts—a spherical term and the corresponding ellipsoidal correction. Similarly, the ellipsoidal solution for the downward continuation of gravity anomalies (see also Section 4) can be found in Martinec and Grafarend (1997). It is expressed as a spherical Poissons kernel plus corrections due to the ellipticity of the boundary. Arguably, the ellipsoidal formulas suffer from smaller approximation errors than the spherical formulas. However, considering the accuracy and the resolution of the presently available topographical data, the possible improvement when incorporating the ellipsoidal approximation most likely does not exceed a cm-level (see also Novák and Grafarend, 2005). Therefore, to avoid cumbersome algebraic manipulations the present UNB approach confines itself to the case of the spherical approximation of the topographic effects. It cannot be excluded, however, that when the more accurate topographic/gravity data becomes available, then at the future developments of the UNB approach the ellipsoidal corrections as discussed in Novák and Grafarend (2005), Martinec and Grafarend (1997) can be considered.

The normal heights are used for estimating the normal gravity in Eqs. (6) and (17). If the orthometric heights are used rather than normal heights, then the so-called "geoid-quasigeoid correction" has to be applied to the boundary condition, Eq. (16) and also in Eq. (17). For a more extended discussion on the ellipsoidal corrections and geoid-quasigeoid correction see Vaníček et al. (1999). The detailed derivation and complete expressions of the atmospheric effects can be found in Novák (2000). The magnitude of the non-topographic corrections comprises only a fraction of the topographic effects. Therefore, to save space, only the expressions for the topographic effects will be presented in the next section. However, in the precise geoid computations the non-topographic effects cannot be ignored.

3. Treatment of the topographic effects

This section focuses on the assessment of the topographic effects, which is the most demanding task in precise geoid determination. First of all, the topographical effects need to be formulated (and evaluated) in its spherical form, instead of widely used planar approximation. It is concluded by Vaníček et al. (2001) that the spherical model is theoretically more correct and should be used whenever a higher accuracy is required. The error in the geoidal heights for the spherical approximation (i.e. $r_g(\Omega) = R$, where R is the mean radius of the Earth) of topography does not exceed 1.5 mm, which is certainly negligible in the practical computations. The spherical model is closer to reality, whereas the planar model does not allow us to use any of the physically meaningful condensation models. Consequently the planar models disqualify for the harmonization of the Earth's gravity field.

The Newton integral can be used for estimating the potential of the topographical masses. Further on, in the computations of Newton's integral it can be split into the Bouguer shell attraction, and the spherical roughness term. This approach has been introduced to eliminate the singularity which may occur in the vicinity of the computation points when integrating with high-resolution datasets. The potential of the topographical masses can be estimated (Martinec, 1993) as

$$
\begin{aligned}
V^{\mathrm{t}}(r_{\mathrm{t}}, \Omega) = {} & 4\pi G\rho_{\mathrm{o}} \frac{R^2}{r_{\mathrm{t}}(\Omega)} H^{\mathrm{O}}(\Omega) \left[1 + \frac{H^{\mathrm{O}}(\Omega)}{R} + \frac{1}{3}\left(\frac{H^{\mathrm{O}}(\Omega)}{R}\right)^2\right] \\
& + G\rho_{\mathrm{o}} \iint_{\Omega' \in \Omega_{\mathrm{O}}} \int_{r'=R+H^{\mathrm{O}}(\Omega')}^{R+H^{\mathrm{O}}(\Omega)} l^{-1}[r_{\mathrm{t}}(\Omega), \psi(\Omega, \Omega'), r'] r'^2 \, \mathrm{d}r' \, \mathrm{d}\Omega' \\
& + G \iint_{\Omega' \in \Omega_{\mathrm{O}}} \delta\rho(\Omega') \int_{r'=R}^{R+H^{\mathrm{O}}(\Omega')} l^{-1}[r_{\mathrm{t}}(\Omega), \psi(\Omega, \Omega'), r'] r'^2 \, \mathrm{d}r' \, \mathrm{d}\Omega'. \qquad (18)
\end{aligned}
$$

where G is the gravitational constant, $l[r_t(\Omega), \psi(\Omega, \Omega'), r']$ and $\psi(\Omega, \Omega')$ are spatial distance and geocentric angle between the computation and integration points, respectively; $d\Omega'$ is the area of the integration element. The first term on the right-hand side of Eq. (18) is the gravitational potential of the spherical Bouguer shell (of mean density ρ_o and thickness equal to the orthometric height $H^O(\Omega)$ of the computation point), see Wichiencharoen (1982). The second term stands for the gravitational potential of the spherical roughness term and the third term represents the effect of the anomalous topographical density $\delta\rho(\Omega)$ distribution on the gravitational potential.

Similarly, the potential of the condensation masses can be written (Martinec, 1993)

$$\begin{aligned} V^{ct}(r_t, \Omega) = {} & 4\pi G\rho_o \frac{R^2}{r_t(\Omega)} H^O(\Omega) \left[1 + \frac{H^O(\Omega)}{R} + \frac{1}{3}\left(\frac{H^O(\Omega)}{R}\right)^2\right] \\ & + G\rho_o \iint_{\Omega' \in \Omega_O} \frac{r_t^3(\Omega') - r_t^3(\Omega)}{3} l^{-1}\left[r_t, \psi(\Omega, \Omega'), R\right] \, d\Omega' \\ & + G \iint_{\Omega' \in \Omega_O} \delta\rho(\Omega') \frac{r_t^3(\Omega') - R^3}{3} l^{-1}[r_t, \psi(\Omega, \Omega'), R] \, d\Omega', \end{aligned} \tag{19}$$

where the first term on the right-hand side is the gravitational potential of the condensed spherical material single layer, the second term stands for the gravitational potential of the spherical roughness term of the condensed topographical masses, and the third term represents the effect of the anomalous condensed topographical density distribution on the gravitational potential.

The secondary indirect topographic effect (the third term on the right-hand side of Eq. (17)) is computed by subtracting Eq. (19) from Eq. (18), i.e.

$$\frac{2}{r_t(\Omega)} \delta V^t(r_t, \Omega) = \frac{2}{r_t(\Omega)} [V^t(r_t, \Omega) - V^{ct}(r_t, \Omega)]. \tag{20}$$

The direct topographic effect is obtained by taking the difference of the radial derivatives of Eqs. (18) and (19). The attraction of the topographical masses reads (Martinec and Vaníček, 1994; Martinec, 1998)

$$\begin{aligned} \left.\frac{\partial V^t(r, \Omega)}{\partial r}\right|_{r=r_t(\Omega)} = {} & -4\pi G\rho_o \frac{R^2}{r_t^2(\Omega)} H^O(\Omega) \left[1 + \frac{H^O(\Omega)}{R} + \frac{1}{3}\left(\frac{H^O(\Omega)}{R}\right)^2\right] \\ & + G\rho_o \iint_{\Omega' \in \Omega_O} \int_{r'=R+H^O(\Omega')}^{R+H^O(\Omega)} \left.\frac{\partial l^{-1}[r, \psi(\Omega, \Omega'), r']}{\partial r}\right|_{r=r_t(\Omega)} r'^2 \, dr' \, d\Omega' \\ & + G \iint_{\Omega' \in \Omega_O} \delta\rho(\Omega') \int_{r'=R}^{R+H^O(\Omega')} \left.\frac{\partial l^{-1}[r, \psi(\Omega, \Omega'), r']}{\partial r}\right|_{r=r_t(\Omega)} r'^2 \, dr' \, d\Omega'. \end{aligned} \tag{21}$$

The first term on the right-hand side is the (negative) gravitational attraction of the spherical Bouguer shell. The second term stands for the gravitational attraction of the spherical roughness term, i.e. the spherical terrain correction, and the third term represents the effect of the anomalous topographical density $\delta\rho(\Omega)$ on the gravitational attraction.

Correspondingly, the attraction of the condensation masses can be expressed (Martinec, 1993)

$$\begin{aligned} \left.\frac{\partial V^{ct}(r, \Omega)}{\partial r}\right|_{r=r_t} = {} & -4\pi G\rho_o \frac{R^2}{r_t^2(\Omega)} H^O(\Omega) \left[1 + \frac{H^O(\Omega)}{R} + \frac{1}{3}\left(\frac{H^O(\Omega)}{R}\right)^2\right] \\ & + G\rho_o \iint_{\Omega' \in \Omega_O} \frac{r_t^3(\Omega') - r_t^3(\Omega)}{3} \left.\frac{\partial l^{-1}[r, \psi(\Omega, \Omega'), R]}{\partial r}\right|_{r=r_t(\Omega)} d\Omega' \\ & + G \iint_{\Omega' \in \Omega_O} \delta\rho(\Omega') \frac{r_t^3(\Omega') - R^3}{3} \left.\frac{\partial l^{-1}[r, \psi(\Omega, \Omega'), R]}{\partial r}\right|_{r=r_t(\Omega)} d\Omega', \end{aligned} \tag{22}$$

where the first term on the right-hand side is the gravitational attraction of the condensed spherical Bouguer shell, the second term stands for the gravitational attraction of the spherical roughness term of the condensed topographical

masses, and the third term represents the effect of the anomalous condensed topographical density distribution on the gravitational attraction.

Note that the first terms of Eqs. (21) and (22) are equal. Thus, the Bouguer shell contributions cancel each other out. The final expression for the direct topographic effect in the Helmert space then becomes:

$$\begin{aligned}\delta A^{\mathrm{t}}(r_{\mathrm{t}},\Omega) = \frac{\partial\{V^{\mathrm{t}}(r_{\mathrm{t}},\Omega)-V^{\mathrm{ct}}(r_{\mathrm{t}},\Omega)\}}{\partial r} &= G\rho_{\mathrm{o}}\iint_{\Omega'\in\Omega_{\mathrm{O}}}\int_{R+H(\Omega)}^{R+H(\Omega')}\frac{\partial l^{-1}\left[r,\psi\left(\Omega,\Omega'\right),r'\right]}{\partial r}\bigg|_{r=r_{\mathrm{t}}(\Omega)} r'^{2}\,\mathrm{d}r'\,\mathrm{d}\Omega' \\ &- G\,\rho_{\mathrm{o}}\iint_{\Omega'\in\Omega_{\mathrm{O}}}\frac{r_{\mathrm{t}}^{3}(\Omega)-r^{3}(\Omega')}{3}\frac{\partial l^{-1}[r,\psi(\Omega,\Omega'),R]}{\partial r}\bigg|_{r=r_{\mathrm{t}}(\Omega)}\mathrm{d}\Omega' \\ &+ G\iint_{\Omega'\in\Omega_{\mathrm{O}}}\int_{R}^{R+H(\Omega')}\delta\rho(\Omega')\frac{\partial l^{-1}[r,\psi(\Omega,\Omega'),r']}{\partial r}\bigg|_{r=r_{\mathrm{t}}(\Omega)} r'^{2}\,\mathrm{d}r'\,\mathrm{d}\Omega' \\ &- G\iint_{\Omega'\in\Omega_{\mathrm{O}}}\delta\rho(\Omega')\frac{r_{\mathrm{t}}^{3}(\Omega)-R^{3}}{3}\frac{\partial l^{-1}[r,\psi(\Omega,\Omega'),R]}{\partial r}\bigg|_{r=r_{\mathrm{t}}(\Omega)}\mathrm{d}\Omega'. \end{aligned} \tag{23}$$

The first term on the right-hand side of Eq. (23) is the so-called "spherical terrain correction", and the second term stands for the "spherical condensed terrain correction" (Martinec and Vaníček, 1994). The third and fourth terms represent together the contribution of the laterally varying topographical density to the direct topographic effect.

The direct and secondary indirect topographic effects are evaluated at the Earth's surface. There is another topographic effect, which must be accounted for on the geoid level. As already noted, the condensation of the atmospheric/topographic masses causes the Helmert potential $W^{\mathrm{h}}(r,\Omega)$ to become slightly different from the actual potential. Consequently, also the Helmert co-geoid does not exactly coincide with the geoid in the real space, see Fig. 1. The effect causing this change is called primary indirect topographic effect (PITE). An important advantage of the Helmert second condensation method is that PITE is nowhere larger than 2 m worldwide (the primary indirect atmospheric effect is <1 cm, globally). PITE can be accounted for as a separate correction to the Helmert co-geoid, which is to be obtained from solving the Stokes boundary value problem. In other words, PITE is the transformation term added to the geoid in Helmert's space to obtain the geoid in the real space.

PITE is computed from the gravitational potentials of the topographical and condensed masses, both referred to the geoid level. The final expression for the PITE is as follows (Martinec, 1993)

$$\begin{aligned}\frac{\delta V^{\mathrm{t}}(R,\Omega)}{\gamma_{\mathrm{o}}(\phi)} &= -4\pi G\rho_{\mathrm{o}}\frac{[H^{\mathrm{O}}(\Omega)]^{2}}{\gamma_{\mathrm{o}}(\phi)}\left[\frac{1}{2}+\frac{H^{\mathrm{O}}(\Omega)}{3R}\right]+\frac{G}{\gamma_{\mathrm{o}}(\phi)}\rho_{\mathrm{o}} \\ &\times\iint_{\Omega'\in\Omega_{\mathrm{O}}}\int_{r'=R+H^{\mathrm{O}}(\Omega)}^{R+H^{\mathrm{O}}(\Omega')} l^{-1}[R,\psi(\Omega,\Omega'),r']r'^{2}\,\mathrm{d}r'\,\mathrm{d}\Omega' \\ &- \frac{G}{\gamma_{\mathrm{o}}(\phi)}\rho_{\mathrm{o}}\iint_{\Omega'\in\Omega_{\mathrm{O}}}\frac{r_{\mathrm{t}}^{3}(\Omega')-r_{\mathrm{t}}^{3}(\Omega)}{3}l^{-1}[R,\psi(\Omega,\Omega'),R]\,\mathrm{d}\Omega' \\ &+ \frac{G}{\gamma_{\mathrm{o}}(\phi)}\iint_{\Omega'\in\Omega_{\mathrm{O}}}\delta\rho(\Omega')\int_{r'=R}^{R+H^{\mathrm{O}}(\Omega')} l^{-1}[R,\psi\left(\Omega,\Omega'\right),r']r'^{2}\,\mathrm{d}r'\,\mathrm{d}\Omega' \\ &- \frac{G}{\gamma_{\mathrm{o}}(\phi)}\iint_{\Omega'\in\Omega_{\mathrm{O}}}\delta\rho(\Omega')\frac{r_{\mathrm{t}}^{3}(\Omega')-R^{3}}{3}l^{-1}[R,\psi(\Omega,\Omega'),R]\,\mathrm{d}\Omega'. \end{aligned} \tag{24}$$

4. Downward continuation of gravity anomalies

Once the Helmert gravity anomaly field is evaluated on the Earth's surface it has to be continued downward or upward to the geoid. At the UNB the downward continuation is solved by using the Poisson integral equation (Heiskanen and

Moritz, 1967, p. 317). This equation had been originally designed as a formula for the upward continuation of harmonic quantities. It can be written as (Kellogg, 1929)

$$\Delta g^{\mathrm{h}}(r_{\mathrm{t}}, \Omega) = \frac{R}{4\pi r_{\mathrm{t}}(\Omega)} \iint_{\Omega' \in \Omega_{\mathrm{O}}} K[r_{\mathrm{t}}(\Omega), \psi(\Omega, \Omega'), R]\, \Delta g^{\mathrm{h}}(r_{\mathrm{g}}, \Omega')\, \mathrm{d}\Omega', \tag{25}$$

where $\mathrm{K}[r_{\mathrm{t}}(\Omega), \psi(\Omega, \Omega'), R]$ is the spherical Poisson integral kernel (e.g. Sun and Vaníček, 1998). Eq. (25), taken as an integral equation, can be re-written as system of linear equations. In the matrix-vector form, it can be presented as follows (Martinec, 1996; Huang, 2002)

$$\Delta \mathbf{g}^{\mathrm{h}}(r_{\mathrm{t}}, \Omega) = \mathbf{K}[r_{\mathrm{t}}(\Omega), \psi(\Omega, \Omega'), R] \Delta \mathbf{g}^{\mathrm{h}}(r_{\mathrm{g}}, \Omega'), \tag{26}$$

where $\Delta \mathbf{g}^{\mathrm{h}}(r_{\mathrm{t}}, \Omega)$ is the vector of the gravity anomalies referred to the Earth's surface, $\Delta \mathbf{g}^{\mathrm{h}}(r_{\mathrm{t}}, \Omega')$ the vector of the gravity anomalies referred to the geoid surface and $\mathbf{K}[r_{\mathrm{t}}(\Omega), \psi(\Omega, \Omega'), R]$ is the matrix of the values of the Poisson integral kernel multiplied by the remaining elements of the right-hand side of Eq. (25).

Downward continuation is an inverse problem to the original Poisson integral. The matrix-vector form of the Poisson integral equation can then be used for solving the inverse problem, i.e. computing the unknown elements of the vector $\Delta \mathbf{g}^{\mathrm{h}}(r_{\mathrm{t}}, \Omega)$. For more details the interested reader is referred to (Sun and Vaníček, 1998; Vaníček et al., 1996a).

As the result of the discretization the Poisson downward continuation is known to be an unstable problem. Due to the instability, existing errors in $\Delta \mathbf{g}^{\mathrm{h}}(r_{\mathrm{t}}, \Omega)$ may appear magnified in the solution. However, when mean values are used instead of point values, this problem is somewhat alleviated, as the mean values do not exhibit the highest frequencies.

5. Solution to Stokes's boundary value problem

The gravity anomalies over the entire Earth are required for the geoid determination by the original Stokes formula. In practice, however, the area of availability of anomalies, i.e. the area of integration is limited to some domain (Ω_{ψ_0}) around the computation point, usually circular. The truncation bias that occurs when the remote zone ($\Omega_0 - \Omega_{\psi_0}$) is neglected in the integration, can be reduced by modifying Stokes's formula (Molodensky et al., 1960). In the UNB approach this problem is remedied by employing the generalized Stokes scheme, which uses the low-frequency part of the geoid described by a global geopotential model, a spheroid of degree M, as a new reference surface (Vaníček and Sjöberg, 1991) instead of the Somigliana–Pizzeti type reference ellipsoid:

$$\begin{aligned} N(\Omega) = {} & \frac{R}{4\pi\gamma_0(\phi)} \iint_{\Omega_{\psi_0}} S^M(\psi_0, \psi(\Omega, \Omega')) \left(\Delta g^{\mathrm{h}}(r_{\mathrm{g}}, \Omega) - \sum_{n=2}^{M} \Delta g_n^{\mathrm{h}}(r_{\mathrm{g}}, \Omega) \right) \mathrm{d}\Omega' \\ & + \frac{R}{2\gamma_0(\phi)} \sum_{n=2}^{M} \frac{2}{n-1} \Delta g_n^{\mathrm{h}}(r_{\mathrm{g}}, \Omega) + \frac{\delta V^{\mathrm{t}}(r_{\mathrm{g}}, \Omega)}{\gamma_0(\phi)}, \end{aligned} \tag{27}$$

where the modified Stokes function $S^M(\psi_0, \psi(\Omega, \Omega'))$ can be computed according to Vaníček and Kleusberg (1987). The modification limit M is selected by diverse criteria which will be discussed later in Section 6. An interesting study on this matter can also be found in Vaníček and Featherstone (1998). Ideally, the modified Stokes formula should lead to the point when the truncation bias can be safely neglected. However, if either the limit M or the radius of the integration cap ψ_0 are too small (or both are too small), then a notable truncation bias may still be present. In principle, this contribution can be accounted for separately by adding the term $R/(2\gamma_0(\phi)) \sum_{M+1}^{120} Q_n^M(\psi_0) \Delta g_n^{\mathrm{h}}(r_{\mathrm{g}}, \Omega)$, where the set of modified truncation coefficients $Q_n^M(\psi_0)$ is a function of the radius ψ_0 of the integration cap. This approach was developed by Martinec (1993), see also Novák et al. (2001).

Some aspects of the usage of the terrestrial gravity anomalies in the generalized Stokes scheme, Eq. (27), need to be emphasized. Recall, that the normal gravity in Eq. (6) for computing the terrestrial gravity anomalies is evaluated applying Somigliana–Pizzeti's theory (and corresponding level ellipsoid) of the normal gravity field (Somigliana, 1930). However, for solving the boundary value problem we abandon this classical concept. Instead of relating the reference quantities to the usual Somigliana–Pizzeti normal (ellipsoidal) field, we take another reference field to convert these standard gravity anomalies into the geoidal heights. The UNB application uses the satellite-only segment of a global geopotential model as a reference spheroid (instead of the usual reference ellipsoid). Rigorously, the quantities within the first right-hand term of Eq. (27) are related to two different reference surfaces. However, since the Stokesian

integration is produced over a limited spatial domain then the inconsistency of the integral arguments is only formal, and the corresponding (numerical) effect on the geoidal height is negligible. For more detailed discussion on these (and related) matters see Vaníček and Sjöberg (1991).

Since a GGM is represented by an external-type series of spherical harmonics, then inside the topographical masses the GGM-deduced gravity quantities may be biased. A correction accounting for this bias has to be introduced. The transformation of the original geopotential coefficients into the Helmert space can be achieved by subtracting the spherical harmonic coefficients of the residual topographic potential (δV_{nm}^{t}) from the corresponding geopotential coefficients (Vaníček et al., 1995). Also the corresponding direct topographical effect should be accounted for. So Helmertised geopotential coefficients need to be used for computing the harmonics $\Delta g_n^h(r_g, \Omega)$ in Eq. (27). Also the differences between the defining constants (i.e. gravity-mass constant, and the major semi-axis of the ellipsoid versus reference radius for the spherical GGM) of the used GGM and adopted geodetic reference ellipsoid need to be considered. This scale change can be introduced via zonal harmonics of the reference ellipsoid by an approach described in Vaníček and Kleusberg (1987, Sect. 5).

The estimator, Eq. (27), employs the high-degree residual gravity anomalies, which are obtained by subtracting the long-wavelength contribution (called as reference gravity anomaly) from the complete gravity anomaly. The Stokesian integration with these Helmert's residual anomalies (i.e. the first term on the right-hand side of Eq. (27)) results in the Helmert residual co-geoid. Since the low-degree reference gravity field is removed from the anomalies before the Stokes integration, the long-wavelength contribution to the geoidal height (see Heiskanen and Moritz, 1967, p. 97), i.e. the reference spheroid, must be added to the residual geoid. The result is called the Helmert co-geoid.

As it was already noted, the Stokes–Helmert approach uses the gravity anomalies on the Helmert *co-geoid* as input to the Stokesian integration. The last term (PITE) in the right-hand side of Eq. (27) transfers the Helmert geoidal heights back into the real space.

This completes the brief review of the theoretical principles of the UNB application of Stokes–Helmert's approach to geoid computation. For more details the interested reader is referred to the relevant publications (see the reference list).

6. Numerical investigations

Over the past years the theory behind the UNB approach has been empirically validated by a number of practical geoid computations, e.g. Vaníček and Kleusberg (1987), Vaníček et al. (1991), Vaníček et al. (1996b), just to name a few.

In previous decades, the geodesists had to overcome the limited capacities (first of all—speed and storage space!) of the computers by introducing certain computational "shortcuts". Fortunately, up-to-date computational possibilities have approached the level, where even the most demanding geoid computational tasks can be fulfilled within reasonable time-period; and more importantly, without unnecessary approximations. Even though the theoretical principles of the UNB geoid determination are rather straightforward, one still needs to make a number of decisions while setting up the actual computations. At this, obviously, the main constraints are the quality and resolution of the available gravimetric and topographic data. One possible scenario for applying the UNB geoid determination methods will be discussed below. It should be emphasized, however, that the content of the present section can only be considered as general guidelines, rather than strict numerical recipes. The reader is encouraged to develop his/her own strategies depending on the available data (and their characteristics).

Recently, a new geoid model was computed over our traditional "playground"—the Canadian Rocky Mountains. The limits of our "playground" are $48^\circ\text{N} < \varphi < 61^\circ\text{N}$; $228^\circ\text{E} < \lambda < 250^\circ\text{E}$, see Fig. 2. This area appears to be the most challenging for testing the geoid modeling strategies, since the highest peaks exceed 2.5 km (an illustration can be found in Janák and Vaníček, 2005, Fig. 3; or Vaníček et al., 1999, Fig. 6) and the gravity field is fairly complicated.

Note that the gravity anomalies from a more extended area are needed for the Stokesian integration (our usual practice is to use a 6° radius for the integration cap). In this way the same geoid modeling conditions are used all over the target area, and the edge effect is eliminated. The topographical effects are evaluated by the expressions in Section 3. Recall that these approaches eliminate the Bouguer shell contribution, abating thus the singularity problem which otherwise would occur at the vicinity of the computation point. For the estimation of the topographic effects the integration domain is divided among different element sizes, with small as possible elements close to the computation point. $3'' \times 3''$ heights are used for the innermost computation zone, $30'' \times 30''$ and $5' \times 5'$ DTM-s for the 5° near-zone, the far-zone (global) contribution is based on $30' \times 30'$ global DTM. The topographic data was supplied by the Geodetic Survey Division of Natural Resources Canada. The topographical effects were computed on a regular grid with a spatial

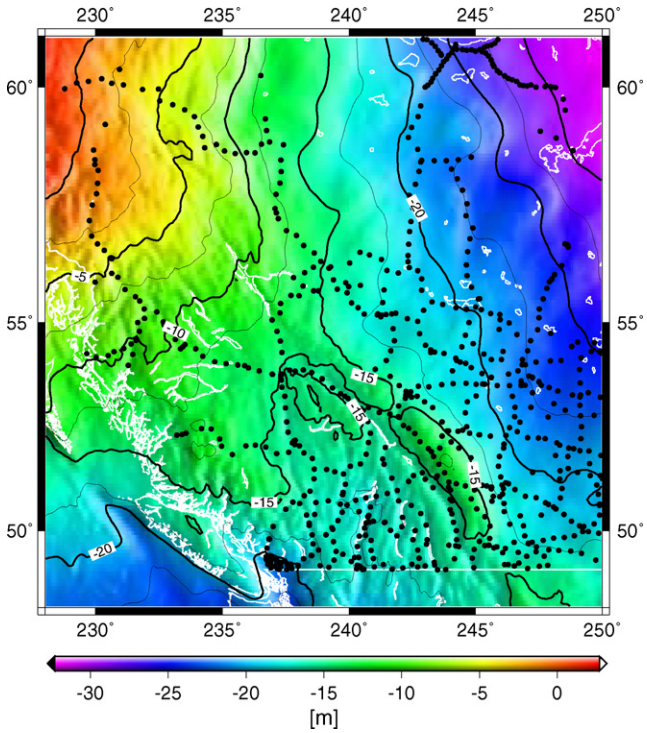

Fig. 2. A UNB geoid model. The modification degree of the modified Stokes function is $M = 60$. Black dots denote the location of the GPS-levelling points. The contour interval is 2.5 m.

resolution of $5' \times 5'$. The mean surface Helmert anomalies were computed at the same grid-points according to Eq. (17). A strategy for computing the mean anomalies from point values can be found in Janák and Vaníček (2005).

Obviously, the regional geoid models are also dependent, among other factors, on the quality of the used GGM. Ongoing and future dedicated gravity missions (i.e. CHAMP, GRACE and GOCE) have enhanced and will enhance the global gravity information significantly. One of the reasons for initiating the study described here was to check the performance of the new geopotential model EIGEN-GRACE02S (Reigber et al., 2005). One hundred and ten days of the GRACE twin-satellites tracking data are the basis of this GGM. The EIGEN-GRACE02S "satellite-only" field is developed up to degree/order 150/150. The authors estimate an 1 cm accuracy in geoid modeling with a spectral resolution up to degree/order 75/75. For more details see the original publication.

The selection of the upper limit, M, for the reference spheroid/anomaly and the modified Stokes function, $S^M(\psi_0, \psi(\Omega, \Omega'))$, is important in geoid modeling. The improved accuracy of up-to-date GGM-s allows the user to increase the degree of the harmonics to be used for regional geoid determination. Due to limited accuracy of the earlier GGM-s a rather small M was favoured in the computations of our past geoid models. For instance, our earlier Canadian geoid models (Vaníček and Kleusberg, 1987; Vaníček et al., 1996b) utilize $M = 20$. Consequently, in these computations even the intermediate wavelength information from a GGM is prevented from affecting the solution. There is another aspect when choosing the limit M for the real data. Recall that the high-degree GGM-s are determined from a combination of satellite data and terrestrial gravity data. This combination implies that the two data sets are correlated with each other. This suggests using the "satellite-only" harmonics for computing the reference quantities in Eq. (27) is a correct way to go.

However, the user of a GGM should not consider the "satellite-only" harmonics as an errorless dataset, especially at the higher degrees. Therefore, one cannot increase the modification limit in Eq. (27) all the way up to maximum available spherical harmonic degree. In this study we experiment with different modification degrees, but never exceeding $M = 60$, which corresponds more or less to the reliability of the EIGEN-GRACE02S. In the selected test area the regional geoid models employing $M = 60$ showed slightly better agreement with GPS-levelling data, than the ones utilizing smaller modification limits. The further details of these experiments are spared for a forthcoming paper.

Since the focus of this paper is summarizing the main theoretical principles of the UNB geoid determination approach then the further discussion of the numerical outcome of different effects is considered outside the scope of the present contribution. This is supported by the fact that the numerical results of the present study generally resemble those of the previous years over the same test area and they can found in the open literature, e.g. see the reference list.

Traditionally, the accuracy of the regional geoid modeling has been validated empirically by using GPS-levelling points. The total number of GPS-levelling points available for the evaluation of the gravimetric geoid model in our area of interest is 726. Their location and the final geoid model are shown in Fig. 2. The gravimetric geoid model was fitted to the GPS-levelling points by a four-parameter polynomial fit to eliminate any secular errors in the geoid. The best achieved RMS error of post-fit residuals was 15 cm. Basically, there are many different approaches for fitting a surface to randomly distributed point-data. The specifics of the fitting procedure employed in this study can be found in Ellmann (2004, pp. 46–48). It should be emphasized that by no means our fit of the gravimetric geoid to the GPS-levelling data can be considered as a "combined adjustment" of the two datasets (cf., e.g. Kotsakis and Sideris, 1999). Besides, the newly "fitted" surface has no physical meaning at all, as opposed to the geoid. Therefore, such fitting procedure has only a secondary interest and it is not considered to be a part of the UNB geoid determination approach. Nevertheless, the increasing demand of using the geoid models for practical (engineering) applications may urge us in future to develop rigorous fitting methods between the two data sets.

As already mentioned, detail discussion on comparing the gravimetric geoid model and GPS-levelling data is not relevant to the main scope of the present paper. However, based on the distribution (not shown here) and magnitude of the post-fit residuals some preliminary conclusions can be made. As expected, the largest post-fit residuals are in the mountainous areas. The pattern of discrepancies is of short-wavelength nature; therefore the new reference model cannot provide significant improvements over such areas. There could be several reasons for these larger discrepancies. Most likely, the problems stem from the estimation of the topographical effects or downward continuation, or both. Furthermore, the discretization error (i.e. due to averaging of point values) cannot be excluded. As it is demonstrated by Janák and Vaníček (2005), that different discretizaton strategies may have a significant effect on the geoidal heights.

It should also be noted that for the sake of simplicity the variations of the topographical density were not considered. However, a numerical study by Huang et al. (2001) demonstrates that the effect of the lateral topographical mass density variation on the geoid height could approach ∼7 cm in this region. Therefore, this effect should also be accounted for very carefully.

So far we have been using $5' \times 5'$ mean gravity anomalies for computing the geoid models of the same resolution. A denser dataset could provide better results. This is supported by Huang and Veronneau (2005), who reported on achieving the standard deviation of the post–fit residuals as 8 cm over almost the same data area. The spatial resolution of their geoid model is $2' \times 2'$. On the other hand, the downward continuation is known to be an unstable problem. Switching from the usual $5' \times 5'$ data resolution into a denser dataset may increase the numerical instability of the solution. A complex investigation of these matters is still in progress and will be reported on in proper time.

Regrettably, the GPS-levelling control points can be found only over the continental areas and their distribution is rather inhomogeneous. Also the systematic biases in the definition of the vertical datum may affect the numerical results. Thus, a reliable synthetic geoid model would be a better candidate for testing the accuracy of the geoid determination methods. Presently, we are testing the UNB approach to geoid computation by using a high-resolution Australian Synthetic Earth Gravity Model (AUS-SEGM, Baran et al., 2006), which became available recently. The results of this work will be given in a forthcoming paper.

7. Summary

This paper summarizes the main theoretical principles of the UNB application of Stokes–Helmert approach to geoid computation. Our approach uses a two-space set-up. Correspondingly, the boundary value problems were formulated for the space of the actual gravity (real space) and for the Helmert space. To achieve the harmonicity of the Helmert anomalies to be downward continued to the geoid level the topographical effects need to be rigorously formulated and evaluated for the spherical Earth. Rigorous treatment of the topographical effects is the backbone of our approach. The formulas for the evaluation of the topographic effects were explicitly spelled out in Section 3. The effects are formulated in their spherical form. Further on, splitting the effects into the contribution of the Bouguer shell and the spherical roughness term leads to the expressions, where the effect of singularity (occurring in the vicinity of the

computation points) is reduced. Our solution of the Stokes boundary value problem is done by means of introducing a reference spheroid of order M and by using the modified Stokes formula.

We think that the UNB approach is theoretically suitable for determining a centimeter-accuracy geoid model, whereas the available terrestrial data coverage and quality allow only a dm-accuracy, at least in the mountainous regions of Canada. This is confirmed also by our latest numerical study, which is discussed in Section 6. In the context of recently released GRACE-based geopotential models also the principles of selecting the appropriate modification limits were revisited.

Acknowledgements

The complete list of individuals whose research has contributed to the UNB approach for the geoid determination can be assembled on the basis of the reference list. We acknowledge the contribution of all these researchers for their effort. We also thank the Canadian Centre of Excellence GEOIDE and the Canadian National Scientific and Engineering Research Council for their sustained financial support. Thoughtful comments made by Prof. Erick Grafarend, the Responsible Editor, and two anonymous reviewers are gratefully acknowledged.

References

Ardalan, A.A., Grafarend, E.W., 2001. Ellipsoidal geoidal undulations (ellipsoidal Bruns formula): case studies. J. Geodesy 75, 544–552.

Baran, I., Kuhn, M., Claessens, S.J., Featherstone, W.F., Holmes, S.A., Vaníček, P., 2006. A synthetic Earth gravity model designed specifically for testing regional gravimetric geoid determination algorithms. J. Geodesy 80, 1–16.

Bruns, H., 1878. Die Figur der Erde. Publikation des Königlichen Preussischen Geodätischen Institutes, Berlin.

Ellmann, A., 2004. The geoid for the Baltic countries determined by the least squares modification of Stokes' formula. Doctoral Dissertation, Geodesy Report No. 1061, Royal Institute of Technology, Department of Infrastructure, Stockholm.

Featherstone, W.F., Holmes, S.A., Kirby, J.F., Kuhn, M., 2004. Comparison of remove-compute-restore and University of New Brunswick techniques to geoid determination over Australia, and inclusion of Wiener-type filters in reference field contribution. J. Surv. Eng. 130, 40–47.

Heiskanen, W.H., Moritz, H., 1967. Physical Geodesy. W.H. Freeman and Co., San Francisco.

Heck, B., 2003. On Helmert's methods of condensation. J. Geodesy 77, 155–170.

Helmert, F.R., 1884. Die mathematischen und physicalishen Theorien der höheren Geodäsie, vol. 2. B.G. Teubner, Leipzig (reprinted in 1962 by Minerva GMBH, Frankfurt/Main).

Huang, J., Vaníček, P., Pagiatakis, S.D., Brink, W., 2001. Effect of topographical density on geoid in the Canadian Rocky Mountains. J. Geodesy 74, 805–815.

Huang, J., 2002. Computational methods for the discrete downward continuation of the Earth gravity and effect of lateral topographical mass density variation on gravity and the geoid. Ph.D. Thesis. University of New Brunswick, Fredericton.

Huang, J., Veronneau, M., 2005. Applications of downward continuation in gravimetric geoid modeling—case studies in Western Canada. J. Geodesy 79, 135–145.

Janák, J., Vaníček, P., 2005. Mean free-air gravity anomalies in the mountains. Studia Geophysica et Geodaetica 49, 31–42.

Jekeli, C., Serpas, J.G., 2003. Review and numerical assessment of the direct topographical reduction in geoid determination. J. Geodesy 77, 226–239.

Kellogg, O.D., 1929. Foundations of Potential Theory. Springer, Berlin.

Kotsakis, C., Sideris, M.G., 1999. On the adjustment of combined GPS/levelling/geoid networks. J. Geodesy 73, 412–421.

Martinec, Z., 1993. Effect of lateral density variations of topographical masses in view of improving geoid model accuracy over Canada. Final Report of the contract DSS No. 23244-2-4356. Geodetic Survey of Canada, Ottawa.

Martinec, Z., Vaníček, P., 1994. Direct topographical effect of Helmert's condensation for a spherical approximation of the geoid. Manuscripta Geodaetica 19, 257–268.

Martinec, Z., 1996. Stability investigations of a discrete downward continuation problem for geoid determination in the Canadian Rocky Mountains. J. Geodesy 70, 805–828.

Martinec, Z., Grafarend, E., 1997. Construction of Green's function to the external Dirichlet boundary-value problem for the Laplace equation on an ellipsoid of revolution. J. Geodesy 71, 562–570.

Martinec, Z., 1998. Boundary Value Problems for Gravimetric Determination of a Precise Geoid. Lecture Notes in Earth Sciences, vol. 73. Springer, Berlin, Heidelberg, New York.

Molodensky, M.S., 1945. Fundamental problems of Geodetic Gravimetry (in Russian). TRUDY TsNIIGAIK 42, Geodezizdat, Moscow.

Molodensky, M.S., Yeremeev, V.F., Yurkina, M.I, 1960. Methods for Study of the External Gravitational Field and Figure of the Earth. TRUDY TsNIIGAiK, 131, Geodezizdat, Moscow. English translat.: Israel Program for Scientific Translation, Jerusalem 1962.

Moritz, H., 1992. Geodetic Reference System 1980. Bull. Géodésique 66, 187–192.

Novák, P., 2000. Evaluation of gravity data for the Stokes–Helmert solution to the geodetic boundary-value problem. Technical Report No. 207, Department of Geodesy and Geomatics Engineering, University of New Brunswick, Fredericton.

Novák, P., Vaníček, P., Martinec, Z., Véronneau, M., 2001. Effect of the spherical terrain on gravity and the geoid. J. Geodesy 75, 491–504.

Novák, P., Grafarend, E.W., 2005. Ellipsoidal representation of the topographical potential and its vertical gradient. J. Geodesy 78, 691–706.
Reigber, C., Schmidt, R., Flechtner, F., König, R., Meyer, U., Neumayer, K.-H., Schwintzer, P., Sheng, Y.Z., 2005. An Earth gravity field model complete to degree and order 150 from GRACE: EIGEN-GRACE02S. J. Geodyn. 39 (1), 1–10.
Sjöberg, L.E., 2005. A discussion on the approximations made in the practical implementation of the remove–compute–restore technique in regional geoid modeling. J. Geodesy 78, 645–653.
Somigliana, C., 1930. Geofisica – Sul campo gravitazionale esterno del geoide ellissoidico. Atti. Reale. Acad. Naz. Lin. Rendi 6, 237–243.
Stokes, G.G., 1849. On the variation of gravity at the surface of the Earth. Trans. Cambridge Philos. Soc. VIIII, 672–695.
Sun, W., Vaníček, P., 1998. On some problems of the downward continuation of the $5' \times 5'$ mean Helmert gravity disturbance. J. Geodesy 72, 411–420.
Vaníček, P., Kleusberg, A., 1987. The Canadian geoid—Stokesian approach. Compilation of a precise regional geoid. Manuscripta Geodaetica 12, 86–98.
Vaníček, P., Sjöberg, L.E., 1991. Reformulation of Stokes's theory for higher than second-degree reference field and modification of integration kernels. J. Geophys. Res. 96 (B4), 6339–6529.
Vaníček, P., Ong, P., Zhang, C., 1991. New gravimetric geoid for Canada: the "UNB90" solution. In: Rapp, R.H., Sanso, F. (Eds.), Determination of the Geoid: Present and Future. Springer, Berlin, pp. 214–219.
Vaníček, P., Martinec, Z., 1994. The Stokes–Helmert scheme for the evaluation of a precise geoid. Manuscripta Geodaetica 19, 119–128.
Vaníček, P., Najafi, M., Martinec, Z., Harrie, L., Sjöberg, L.E., 1995. Higher-degree reference field in the generalised Stokes–Helmert scheme for geoid computation. J. Geodesy 70, 176–182.
Vaníček, P., Sun, W., Ong, P., Martinec, Z., Najafi, M., Vajda, P., Horst, B., 1996a. Downward continuation of Helmert's gravity. J. Geodesy 71, 21–34.
Vaníček, P., Kleusberg, A., Martinec, Z., Sun, W., Ong, P., Najafi, M., Vajda, P., Harrie, L., Tomasek, P., ter Horst, B., 1996b. Compilation of the precise regional geoid. Department of Geodesy and Geomatics Engineering Technical Report No. 184, University of New Brunswick, Fredericton.
Vaníček, P., Featherstone, W.E., 1998. Performance of three types of Stokes's kernel in the combined solution for the geoid. J. Geodesy 72, 684–697.
Vaníček, P., Huang, J., Novák, P., Pagiatakis, S.D., Véronneau, M., Martinec, Z., Featherstone, W.E., 1999. Determination of the boundary values for the Stokes–Helmert problem. J. Geodesy 73, 160–192.
Vaníček, P., Novák, P., Martinec, Z., 2001. Geoid, topography, and the Bouguer plate or shell. J. Geodesy 75, 210–215.
Wichiencharoen, C., 1982. The indirect effects on the computation of geoid undulations. Dept. of Geod. Sci. Report No. 336, Ohio State University, Columbus.